Large-Scale Mapping Observations of the C i (3P1–3P0) and CO (J = 3–2) Lines toward the Orion A Molecular Cloud

LARGE-SCALE MAPPING OBSERVATIONS OF THE C I ($^3P_1$–$^3P_0$) AND CO (J = 3–2) LINES TOWARD THE ORION A MOLECULAR CLOUD

MASAFUMI IKEDA,[1] HIROYUKI MAEZAWA,[1] TETSUYA ITO,[1] GAKU SAITO,[1] YUTARO SEKIMOTO,[1,2] SATOSHI YAMAMOTO,[1] KEN'ICHI TATEMATSU,[3] YUJI ARIKAWA,[3,4] YOSHIYUKI ASO,[3,5] TAKASHI NOGUCHI,[3] SHENG-CAI SHI,[3,6] KEISUKE MIYAZAWA,[3] SHUJI SAITO,[7] HIROYUKI OZEKI,[7,8] HIDEO FUJIWARA,[7,9] MASATOSHI OHISHI,[10] AND JUNJI INATANI[11]

ABSTRACT

Large-scale mapping observations of the $^3P_1$–$^3P_0$ fine-structure transition of atomic carbon (C I, 492 GHz) and the J = 3–2 transition of CO (346 GHz) toward the Orion A molecular cloud have been carried out with the Mount Fuji submillimeter-wave telescope. The observations cover 9 deg^2 and include the Orion Nebula M42 and the L1641 dark cloud complex. The C I emission extends over almost the entire region of the Orion A cloud and is surprisingly similar to that of ^{13}CO (J = 1–0). The CO (J = 3–2) emission shows a more featureless and extended distribution than C I. The C I/CO (J = 3–2) integrated intensity ratio shows a spatial gradient running from the north (0.10) to the south (1.2) of the Orion A cloud, which we interpret as a consequence of the temperature gradient. On the other hand, the C I/^{13}CO (J = 1–0) intensity ratio shows no systematic gradient. We have found a good correlation between the C I and ^{13}CO (J = 1–0) intensities over the Orion A cloud. This result is discussed on the basis of photodissociation region models.

Subject headings: ISM: atoms — ISM: individual (Orion A Cloud) — ISM: molecules

1. INTRODUCTION

Neutral atomic carbon (C I) plays important roles in cooling and chemical processes in interstellar clouds, and its submillimeter-wave transitions ($^3P_1$–$^3P_0$, 492 GHz; $^3P_2$–$^3P_1$, 809 GHz) have been observed toward various objects. The detailed distribution of C I around representative objects including photodissociation regions (PDRs) has been studied at high angular resolution (e.g., Minchin et al. 1994; Tauber et al. 1995; White & Sandell 1995). Since C I is widely distributed throughout our Galaxy according to the data from the *COBE* satellite (Wright et al. 1991), it is of fundamental importance to map its large-scale distribution over molecular clouds. Pioneering studies in this direction have been made using a focal reducer installed on the Caltech Submillimeter Observatory (CSO) 10 m antenna (Plume, Jaffe, & Keene 1994; Plume et al. 1999; Tatematsu et al. 1999) to survey the distribution of C I toward several molecular clouds with a moderate resolution of ~3′. In spite of these efforts, the observed areas are still limited relative to available maps of CO and its isotopomers. With this in mind, we have recently constructed a 1.2 m submillimeter-wave telescope for the exclusive use of C I survey observations at the summit of Mount Fuji.

The Orion A cloud is the nearest giant molecular cloud and is located at about 450 pc from the Sun (Genzel & Stutzki 1989). Extensive observations of the cloud have been made in CO (J = 2–1) (Sakamoto et al. 1994), ^{13}CO (J = 1–0) (Bally et al. 1987; Nagahama et al. 1998), CS (J = 1–0) (Tatematsu et al. 1993), and CS (J = 2–1) (Tatematsu et al. 1998). These observations have revealed that numerous dense cores, some of which are the birthplaces of new stars, are distributed throughout the cloud. The northern part of the Orion A cloud is known to be an active site of massive star formation. As a result, the cloud is illuminated by strong UV radiation from OB stars (G_0 is ~10^5 in the vicinity of Orion-KL). By contrast, the central and southern parts of the Orion A cloud are more quiescent and known as the L1641 dark cloud. Although a number of low-mass protostars, T Tauri stars, and Hα emission-line stars are present, no massive stars are found there, and the UV radiation field is much weaker (G_0 ~ 1–5). Therefore, the Orion A cloud is a good target for studying the structure of a molecular cloud under various UV field strengths.

In contrast to the extensive studies of the molecular gas distribution, only a few mapping observations of C I have been reported toward small portions of the Orion A cloud. White & Padman (1991) and White & Sandell (1995) observed the Orion-KL region with a 9.″8 beam. Tauber et al. (1995) reported a 15″ map of the Orion bright bar and Orion-S cloud. Tatematsu et al. (1999) explored the C I distribution in a part of the J-shaped filament with a focal reducer system on the CSO. In this Letter, we present the first large-scale maps of C I and CO (J = 3–2) covering the entire region of the Orion A cloud.

2. OBSERVATIONS

The C I ($^3P_1$–$^3P_0$) and CO (J = 3–2) data were taken between 1998 December and 1999 March using the Mount Fuji submillimeter-wave telescope. The diameter of the main reflector is 1.2 m, corresponding to a half-power beamwidth of 2.′2 and

[1] Research Center for the Early Universe and Department of Physics, University of Tokyo, Tokyo 113-0033, Japan.
[2] Present address: Nobeyama Radio Observatory, National Astronomical Observatory of Japan.
[3] Nobeyama Radio Observatory, National Astronomical Observatory of Japan, Nagano 384-1305, Japan.
[4] Department of Astronomical Science, the Graduate University for Advanced Studies, Nobeyama Radio Observatory, Nagano 384-1305, Japan.
[5] Department of Astronomy, University of Tokyo, Tokyo 113-0033, Japan.
[6] Present address: Purple Mountain Observatory, Nanjing, JiangSu 210008, China.
[7] Institute for Molecular Science, Okazaki 444-8585, Japan.
[8] Present address: National Space Development Agency of Japan, Tsukuba, Ibaraki 305-8505, Japan.
[9] Present address: Department of Chemical System Engineering, School of Engineering, University of Tokyo, Tokyo 113-0033, Japan.
[10] National Astronomy Observatory of Japan, Mitaka, Tokyo 181-8588, Japan.
[11] National Space Development Agency of Japan, Tsukuba, Ibaraki 305-8505, Japan.

3.1 at 492 and 346 GHz, respectively. The telescope is enclosed in a space frame radome whose transmission efficiency is 0.8 at 492 GHz and 0.9 at 346 GHz. The pointing of the telescope was checked and corrected by observing 346 GHz continuum emission from the Sun and the Moon every month, and the pointing accuracy has been maintained within 20″(rms) during the observing run. We used a 346/492 GHz dual-band SIS mixer receiver in our observations. Typical system temperatures including the atmospheric attenuation were 500 K (double sideband) at 346 GHz and 1500 K (single sideband) at 492 GHz. The back end is a 1024 channel acousto-optical spectrometer which has a total bandwidth of 900 MHz and an effective spectral resolution of 1.6 MHz. We split the spectrometer into two halves, each with 450 MHz bandwidth, to allow simultaneous observations of the C I and CO (J = 3–2) lines. Further details of the telescope will be described elsewhere (Y. Sekimoto et al. 1999, in preparation; Maezawa et al. 1999).

We observed using position switching, where the off-source position was at (α_{1950}, δ_{1950}) = ($05^h28^m46^s.5$, $-05°54'28''.0$) for observations of the northern region and ($05^h32^m00^s.0$, $-07°18'00''.0$) for the southern region, which were free of line emission to an rms noise level of 40 mK in the 1.6 MHz resolution. The intensity scale was calibrated using a chopper-wheel method. The moon efficiency including the radome loss is measured to be 0.75 at 346 GHz and 0.72 at 492 GHz. We will present intensities in the main-beam temperature scale (T_{MB}) throughout this Letter. The line intensities were checked every 4 hr by observing Orion-KL. The overall relative uncertainty in the final intensity scale is estimated to be within 20%. The zenith optical depth at 492 GHz ranged from 0.4 to 1.0 during the observations.

We have observed an ~9 deg^2 area of the Orion A cloud with a grid spacing of 3′. For most positions, the C I and CO (J = 3–2) lines were observed simultaneously. Furthermore, we have taken additional C I data with a grid spacing of 1.′5 for an ~0.9 deg^2 region around Orion-KL and L1641N. In total, 4613 C I spectra and 3087 CO (J = 3–2) spectra were obtained. The on-source integration time ranged from 20 to 40 s per position and yielded typical rms noise temperatures of 0.5 K for CO (J = 3–2) and 0.6 K for C I. In this Letter, we concentrate on the global distributions of C I and CO (J = 3–2).

3. OVERALL DISTRIBUTION OF C I AND CO (J = 3–2)

Figure 1*a* shows the intensity map for C I, integrated between 3 and 13 km s^{-1}. C I emission is detected over almost the entire region of the Orion A cloud. The strongest C I emission is seen toward ($\Delta\alpha$, $\Delta\delta$) = (−40″, −220″) from Orion-KL ($05^h32^m46^s.5$, $-05°24'28''$), where the peak temperature is 14.0 K, and slightly weaker toward Orion-KL. This trend was also seen in the higher resolution beam of White & Sandell (1995). At Orion-KL the peak temperature is 9.1 K, the FWHM line width is 4.4 km s^{-1}, and the peak LSR velocity is 9.4 km s^{-1}, which agree closely with the results reported with a similar beam size by Phillips & Huggins (1981). In the C I map, the ∫-shaped filament reported by Bally et al. (1987) is clearly seen. At the southern end of the ∫-shaped filament, a large dark cloud called L1641N can be identified, which is known to be a formation site of a low-mass cluster (Hodapp & Deane 1993). The peak temperature of C I ranges up to 7 K around this region. From the south of L1641N, a filamentary structure continues to the southern end of the cloud with an almost constant width of about 4.4 pc. The left edge of this filament forms a straight

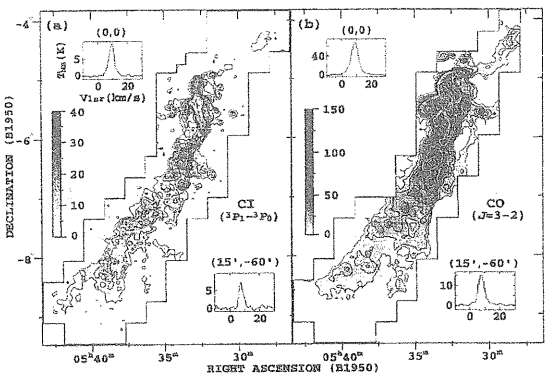

FIG. 1.—Integrated intensity of (*a*) C I ($^3P_1$–$^3P_0$) and (*b*) CO (J = 3–2) observed toward the Orion A cloud over the range 3–13 km s^{-1}. The solid lines enclose the observed region. The contour levels for C I are from 6 to 39 K km s^{-1} with intervals of 3 K km s^{-1}. The contour levels for CO (J = 3–2) are 6, 12, 18, 24, 30, 39, 48, 60, 90, 120, 150, 210, 270, and 330 K km s^{-1}. Spectra observed at offset positions of (0, 0) and (15′, −60′) are also shown in each figure, where (0, 0) corresponds to the central position (α, δ)$_{1950}$ = ($05^h32^m46^s.5$, $-05°24'28''$).

line, and the filament is broken into a number of smaller clumps. The C I intensity decreases toward the south with $T_{MB} \lesssim 3$ K and $\Delta v \sim 2.5$ km s^{-1}, similar to values reported for Heiles Cloud 2 (Maezawa et al. 1999). The overall distribution of the C I emission closely resembles that of ^{13}CO (J = 1–0) by Bally et al. (1987) with a similar (1.′7) beam to the C I observations.

Figure 1*b* shows the integrated intensity map for CO (J = 3–2). The emission peaks at Orion-KL where its T_{MB} equals 67.8 K and the line width Δv is 5.8 km s^{-1}. The line profile of CO (J = 3–2) shows wing emission originating from the molecular outflow, which is not seen in the C I spectra. The CO (J = 3–2) intensity drops sharply away from Orion-KL, and the ∫-shaped filament is less clearly seen than in the C I map. In the central and southern parts of the cloud, the CO (J = 3–2) intensity distribution is rather featureless compared to that of C I. Although the large-scale distribution of CO (J = 3–2) is similar to that of C I, the spatial extent is much larger. These features are probably due to a large optical depth in the CO (J = 3–2) line. Toward the southern part of the Orion A cloud, the T_{MB} of CO (J = 3–2) is typically 3 K and $\Delta v \sim$ 3.0 km s^{-1}, similar to that of the C I line.

4. C I/CO (J = 3–2) INTENSITY RATIO

Figure 2*a* shows a map of the integrated intensity ratio of C I/CO (J = 3–2). The ratio shows a gradient from north to south. Around the Orion-KL region the ratio is as low as 0.10, increasing to 0.29 in L1641N and 1.2 at the southern end of the cloud. The total intensity ratio for the Orion A cloud is evaluated to be 0.37. This value is slightly lower than the value for the Galactic plane, 0.57, reduced to the intensity ratio from the values observed by the *COBE* satellite (Wright et al. 1991).

The C I optical depth has been suggested to be small or moderate (~3) for a wide range of UV fields and densities (Zmuidzinas et al. 1988; Plume et al. 1999). By contrast the optical depth of CO (J = 3–2) is expected to be much larger than that of C I. The C I/CO (J = 3–2) ratio is sensitive to the optical depth of C I if the CO (J = 3–2) line is saturated and the excitation temperatures for both lines are similar. The ob-

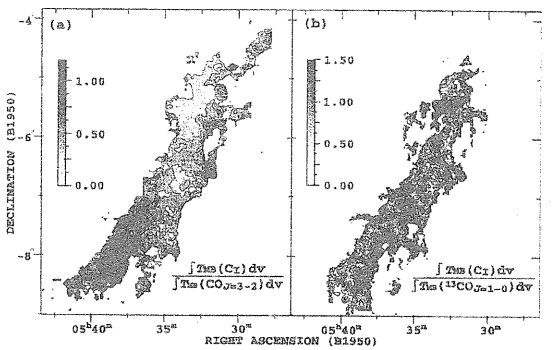

FIG. 2.—(*a*) Ratio of $\int T_{MB}(\mathrm{C\ I})dv$ to $\int T_{MB}$ [CO (J = 3–2)] dv. The contour levels range from 0.1 to 0.9 with intervals of 0.2. (*b*) Ratio of $\int T_{MB}(\mathrm{C\ I})dv$ to $\int T_{MB}$ [^{13}CO (J = 1–0)] dv. The contour levels range from 0.3 to 0.9 with intervals of 0.2. The ^{13}CO (J = 1–0) data was obtained from Bally et al. (1987). The velocity range integrated was from 3 to 13 km s^{-1} for all lines.

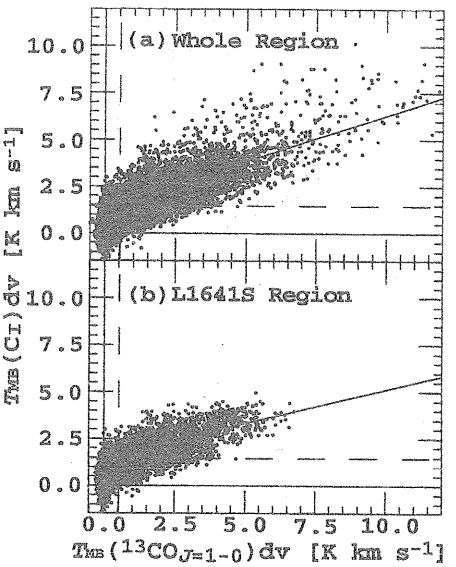

FIG. 3.—Intensities of C I integrated over 1 km s^{-1} bins running from 3 to 13 km s^{-1} are plotted against those of ^{13}CO (J = 1–0). The ^{13}CO (J = 1–0) data is obtained from Bally et al. (1987). The dashed lines show 3 σ levels. The thick solid lines denote linear fits to the data. The data correspond to (*a*) the whole region of the Orion A cloud and (*b*) the L1641S region (below declination −7°.4).

served gradient suggests that τ(C I) increases from the northern to the southern parts. The C I optical depth depends on the excitation temperature and on the column density N(C I). The gas kinetic temperature is known to have a spatial gradient, from 60 K at Orion-KL to ~15 K at the southern end of L1641 (Tatematsu & Wilson 1998). If we assume the LTE condition, the C I optical depth increases by a factor of 6 from north to south with a fixed column density. Thus, the optical depth gradient is likely to reflect the temperature gradient, although a gradient in the C I /CO abundance ratio cannot be ruled out completely.

5. CORRELATION BETWEEN C I AND ^{13}CO (J = 1–0)

Figure 2*b* shows a map of the integrated intensity ratio of C I/^{13}CO (J = 1–0), where the ^{13}CO (J = 1–0) data were taken from Bally et al. (1987). No systematic gradient is seen in this map. If we assume that the ^{13}CO (J = 1–0) line is optically thin for the entire cloud, the C I/^{13}CO (J = 1–0) integrated intensity ratio approximately expresses the optical depth ratio τ(C I)/τ(^{13}CO). Since the column density ratio N(C I)/N(CO) is proportional to the optical depth ratio at a given temperature, our result may suggest an almost uniform N(C I)/N(CO) ratio from north to south along the cloud regardless of the strength of the UV field. In order to confirm this, we derived the column densities of C I and CO under the LTE condition toward several representative positions as shown in Table 1 and find that the N(C I)/N(CO) ratio remains almost constant. However, the ratio along the ridge of the filament tends to be slightly lower than toward the edges. This trend is particularly clear in the ∫-shaped filament and similar to that reported by Plume et al. (1999) for much smaller regions toward W3, NGC 2024, S140, and Cepheus A.

Figure 2*b* also suggests that the integrated intensity of C I correlates well with that of ^{13}CO (J = 1–0). A correlation between C I and ^{13}CO (J = 2–1) intensity has previously been suggested by Tauber et al. (1995) and Tatematsu et al. (1999) toward small portions of the Orion A cloud. Our results show that this correlation holds over an almost entire region of the Orion A cloud. In order to investigate this in detail, we prepared a correlation diagram by integrating the intensities over the 1 km s^{-1} velocity width for the whole Orion A cloud (Fig. 3*a*) and the southern region of the cloud (Fig. 3*b*). The ^{13}CO (J = 1–0) data were smoothed to a 3′ grid for comparison with our C I data. The C I intensity has an offset at zero intensity from ^{13}CO (J = 1–0) and increases almost linearly as the ^{13}CO (J = 1–0) intensity increases. We least-square fitted the following equations: $\int T_{MB}(\mathrm{C\ I})dv = A \int T_{MB}$ [CO(J = 1–0)] $dv + B$,

TABLE 1

TYPICAL LINE PARAMETERS OF C I AND CO (J = 3–2) AND COLUMN DENSITIES OF C I

SOURCE	POSITION ($\Delta\alpha$, $\Delta\delta$)[a]	T_{MB} (K)		Δv (km s^{-1})		$\int T_{MB}\,dv$ (K km s^{-1})		T_{ex}[b] (K)	τ(C I)	N(C I) ($\times 10^{17}$ cm^{-2})	N(CO)[c] ($\times 10^{17}$ cm^{-2})	N(C I)/N(CO)
		C I	CO	C I	CO	C I	CO					
Orion-KL	(0, 0)	9.1	67.8	4.4	5.8	46	475	65.0	0.2	6.2	123	0.05
L1641-N	(15′, −60′)	7.2	15.0	3.3	5.0	25	85	21.6	0.9	3.2	31	0.10
L1641-C	(51′, −102′)	5.4	6.0	2.2	3.7	14.1	25	15.9	1.5	2.1	9.8	0.21
L1641-S4	(90′, −165′)	3.6	3.8	3.2	2.8	13.8	11.4	16.0	0.7	2.0	14.4	0.14

[a] Offsets are relative to the central position (α, δ)$_{1950}$ = (05^{h}32^{m}46^s.5, −05°24′28″).
[b] Taken from Nagahama et al. (1998): T_{ex} for Orion-KL is taken from their Fig. 5 and for other positions from their Table 2.
[c] The column density of CO is calculated from the ^{13}CO (J = 1–0) data (Bally et al. 1987) assuming that CO/^{13}CO is 60 (Langer & Penzias 1993).

where we used the data above the 3 σ noise level for the ^{13}CO (J = 1–0) in this analysis. The coefficients (A, B) are derived to be (0.55 ± 0.02, 0.87 ± 0.04 K km s^{-1}) and (0.46 ± 0.03, 0.92 ± 0.06 K km s^{-1}), and the correlation coefficients are 0.82 and 0.80 for the whole cloud and southern regions, respectively. It should be noted that the C I emission tends to saturate for the larger ^{13}CO (J = 1–0) intensities as seen in Figure 3*b*.

One explanation for these properties can be given in terms of a picture of a PDR. An almost identical C I distribution to that of ^{13}CO (J = 1–0) could not easily be explained by homogeneous PDR models (e.g., Tielens & Hollenbach 1985). Taking this into account, we will assume that the cloud consists of a numerous small clumps, which are exposed to the external UV radiation. In a small clump with low visual extinction, all the CO is destroyed and only C I exists (Monteiro 1991). This may be the reason that the offset in the C I intensity is seen. The H_2 column density of such a clump is estimated from the B constants to be $\sim 1 \times 10^{21}$ cm^{-2}, where the C I abundance is assumed to be 10^{-4} (Suzuki et al. 1992). This corresponds to a visual extinction $A_V \sim 1$, which agrees with the depth of the C I layers in PDR models (e.g., Köster et al. 1994; Spaans 1996). As the clump size increases, CO can exist in the central part of the clump. For larger clumps, the size of the CO core increases, and C I exists only near the clump surface. Therefore, the C I emission tends to saturate for larger ^{13}CO (J = 1–0) intensities.

If the above picture based on the PDR model is correct, the N(C I)/N(CO) ratio should depend on the size distribution of clumps as well as on the UV field intensity. It is therefore curious that the N(C I)/N(CO) ratio shows no such systematic gradient from the northern to the southern part of the Orion A cloud. Considering this fact, the possibility that C I coexists with CO in the deep interior of the cloud should also be considered seriously. Evolutionary models (Suzuki et al. 1992) and chemical bi-stability models (Le Bourlot, des Forêts, & Roueff 1993) may be potential candidates. Further observations including the C I ($^3P_2$–$^3P_1$) line are necessary to characterize physical conditions of the C I–emitting regions, which will be a key to solve the above problem.

We would like to acknowledge John Bally for allowing us to use their ^{13}CO (J = 1–0) data in digital form. We are grateful to Tomoharu Oka for valuable discussions and to Glenn White for his critical reading of the manuscript. This study is supported by Grant-in-Aid from the Ministry of Education, Science, and Culture (07CE2002 and 11304010).

REFERENCES

Bally, J., Langer, W. D., Stark, A. A., & Wilson, R. W. 1987, ApJ, 312, L45
Genzel, R., & Stutzki, J. 1989, ARA&A, 27, 41
Hodapp, K., & Deane, J. 1993, ApJS, 88, 119
Köster, B., Störzer, H., Stutzki, J., & Sternberg, A. 1994, A&A, 284, 545
Langer, W. D., & Penzias, A. A. 1993, ApJ, 408, 539
Le Bourlot, J., des Forêts, G. P., & Roueff, E. 1993, ApJ, 416, L87
Maezawa, H., et al. 1999, ApJ, 524, L129
Minchin, N. R., White, G. J., Stutzki, J., & Krause, D. 1994, A&A, 291, 250
Monteiro, T. T. 1991, A&A, 241, L5
Nagahama, T., Mizuno, A., Ogawa, H., & Fukui, Y. 1998, AJ, 116, 336
Phillips, T. G., & Huggins, P. J. 1981, ApJ, 251, 533
Plume, R., Jaffe, D. T., & Keene, J. 1994, ApJ, 425, L49
Plume, R., Jaffe, D. T., Tatematsu, K., Evans, N. J., II, & Keene, J. 1999, ApJ, 512, 768
Sakamoto, S., Hayashi, M., Hasegawa, T., Handa, T., & Oka, T. 1994, ApJ, 425, 641
Spaans, M. 1996, A&A, 307, 271
Suzuki, H., Yamamoto, S., Ohishi, M., Kaifu, N., Ishikawa, S., Hirahara, Y., & Takano, S. 1992, ApJ, 392, 551
Tatematsu, K., et al. 1993, ApJ, 404, 643
Tatematsu, K., Jaffe, D. T., Plume, R., Evans, N. J., II, & Keene, J. 1999, ApJ, 526, 295
Tatematsu, K., Umemoto, T., Heyer, M. H., Hirano, N., Kameya, O., & Jaffe, D. T. 1998, ApJS, 118, 517
Tatematsu, K., & Wilson, T. L. 1999, in ASP Conf. Ser., The Orion Complex Revisited, ed. M. McCaughrean & A. Burkert (San Francisco: ASP), in press
Tauber, J. A., Lis, D. C., Keene, J., Schilke, P., & Büttgenbach, T. H. 1995, A&A, 297, 567
Tielens, A. G. G. M., & Hollenbach, D. 1985, ApJ, 291, 722
White, G. J., & Padman, R. 1991, Nature, 354, 511
White, G. J., & Sandell, G. 1995, A&A, 299, 179
Wright, E. L., et al. 1991, ApJ, 381, 200
Zmuidzinas, J., Betz, A. L., Boreiko, R. T., & Goldhaber, D. M. 1988, ApJ, 335, 774